Abant Sağlık Bilimleri ve Teknolojileri Dergisi

Abant Journal of Health Sciences and Technologies

2022;2(1):1–9

Body-Mass Recognition and Subdivision With R-CNN Methodology; A Case Study on Pseudocolor Mammograms

R-CNN Metodoloji Vasıtasıyla Kütlelerin Tespit Edilerek Klasifiye Edilmesi; Türetilen Renkli Mamogramlar Üzerine Bir Çalışma

Şükran Yaman Atcı[1], Fatma Kosavalı Çavuş[2]

Geliş Tarihi (*Received*): 12.08.2021 **Kabul Tarihi (*Accepted*):** 23.12.2021 **Yayın Tarihi (*Published*):** 25.06.2022

Öz: Bu çalışma, uzmanlara mamogram görüntülerinde meme kitlelerini tespit etmesine yardımcı olan bir hesaplamalı metodoloji sunmaktadır. Metodolojinin ilk aşaması, mamogram görüntüsünü iyileştirmeyi amaçlar. Bu aşama, memenin dışındaki nesnelerin çıkarılması, gürültünün azaltılması ve memenin iç yapılarının vurgulanmasından oluşur. Daha sonra, hücresel sinir ağları kütle içerebilecek bölgeleri bölümlere ayırmak için kullanılır. Bu sistem dahilinde; Maske R-CNN tabanlı vücut kütlesi tanıma segmentasyonu ile birlikte yönlendirilmiş renk tayfı ön işlemine tutulmuş mammogramlar kullanılmaktadır. Bu bölgelerin şekilleri, şekil tanımlayıcıları analiz edilir ve dokuları jeoistatistik fonksiyonlarla (Ripley's K fonksiyonu ve Moran's ve Geary's indeksleri) analiz edilir. Çok ölçekli morfolojik eleme, Maske R-CNN performansını iyileştirmek için kütle benzeri desenleri artırarak gri tonlamalı mamogramları yönlenmeli renkli resimlere dönüştürür. Genel veri seti üzerinde test edildiğinde, bu çalışma kapsamındaki vakaların ~%65'inin, uygun şekilde ayrılmış veya yayılmış 4687 pikselle temsil edildiği görüldü ve ortalama geçerli bir pozitif oran elde edildi.

Anahtar Kelimeler: Görüntü İşleme, Konvolüsyonlu Sinir Ağı, Mamogram, Meme Kanseri Taraması.

&

Abstract: This study provides a computational methodology that helps experts detect breast masses on mammogram images. The first phase of the methodology aims to improve the mammogram image. This phase consists of removing objects outside the breast, reducing noise, and emphasizing the internal structures of the breast. Then, cellular neural networks are used to compartmentalize regions that may contain mass. Masked R-CNN-based body mass recognition segmentation and guided color spectrum preprocessed mammograms are employed in this approach. The shapes, shape descriptors of these regions are analyzed and their textures are analyzed with geostatistical functions (Ripley's K function and Moran's and Geary's indices). Multiscale morphological screening improves Mask R-CNN performance by converting grayscale mammograms into directed color pictures by boosting mass-like patterns. When tested on the general dataset, ~65% of the cases covered in this study were represented by 4687 pixels appropriately separated or spanned, resulting in an average valid positive rate.

Keywords: Breast Cancer Scanning, Image Process, Mammograms, R-CNN.

Atıf/Cite as: Atcı ŞY., Çavuş FK. Body-Mass Recognition and Subdivision With R-CNN Methodology; A Case Study on Pseudocolor Mammograms. Abant Sağlık Bilimleri ve Teknolojileri Dergisi, 2022;2(1):1-9.

İntihal-Plagiarism/Etik-Ethic: Bu makale, en az iki hakem tarafından incelenmiş ve intihal içermediği, araştırma ve yayın etiğine uyulduğu teyit edilmiştir. / This article has been reviewed by at least two referees and it has been confirmed that it is plagiarism-free and complies with research and publication ethics. https://dergipark.org.tr/tr/pub/sabited/policy

[1] Öğr. Gör. Şükran Yaman Atcı, Haliç Üniversitesi, Meslek Yüksekokulu, Bilgisayar Programcılığı, sukranatci@halic.edu.tr. (Sorumlu yazar.)

[2] Dr. Öğr. Üyesi Fatma Kosovalı Çavuş, Haliç Üniversitesi, Meslek Yüksekokulu, Elektronik Teknolojisi, fatmacavus@halic.edu.tr.

Introduction

Breast cancer is one of the peak communal malignancies in women worldwide (1). Mammography is the most common method of breast screening, although the enormous amount of data collected might cause tiredness and missed detections when analyzed by numerous scientists (2). Computer-aided detection (CAD) systems have been formed as a second pair of eyes' in mammography interpretation to help radiologists boost detection certainty (3,4). A breast mass CAD system typically extracts many area candidates that may contain masses before classifying them as abnormal or regular, depending on the attributes collected from these regions. Traditional CAD's depend on unsupervised area candidate generation and hand-crafted characteristics to identify breast masses (Fig.1; 5,6). However, striking a balance between discriminative strength and robustness might be challenging when utilizing handmade features. Recent advances in deep learning (DL)-based algorithms could give more consistent responses to this dispute. Thus, these approaches have proven effective, which use convolutional neural networks (CNNs) to study evocative features straight from examination data (3). For region candidate suggestion, Saidin et al. and Wang et al. used a multi-scale deep belief network and Gaussian mixture model and then categorized the area candidates using a combination of R-CNN and random forests (7,8). Xu et al. used an unsupervised region proposal approach based on morphological analysis and a CNN to categorize the area candidates (9). These CAD's, on the other hand, locate masses rather than segment them.

A new segmentation step must be introduced to the system to segment masses. Wang et al. added a segmentation approach based on conditional random fields and a level set mechanism to their prior work. However, only true positive (TP) detections are segmented in this study, and false positive (FP) detections must be manually discarded. Body-mass recognition and segmentation are independent tasks requiring several DL networks' sequential tuning. Carneiro et al. and Gan et al. employed a residual neural network (ResNet) to create area candidates and a CNN to categorize them. A segmentation refinement approach generated mass contours (10,11). A better-integrated framework can handle body-mass recognition and segmentation simultaneously is still needed.

In this paper, a fully integrated mammographic is offered with a CAD system that, in a basic framework, can identify and divide masses concurrently without user involvement. As demonstrated in Figure 1, the system has two primary stages: pseudocolor picture creation and detection segmentation based on the Mask R-CNN (12). The notion of pseudocolor mammography (PCM), which shows mass-like patterns with a color contrast concerning the backdrop, is a fundamental contribution of this study. As demonstrated in Figure 2, the PCM is created by adding two morphologically filtered mammograms to the grayscale mammogram in two adjacent picture channels. Due to the restricted quantity of publicly accessible mammographic datasets, transfer learning is used with Mask R-CNN to identify masses on PCMs.

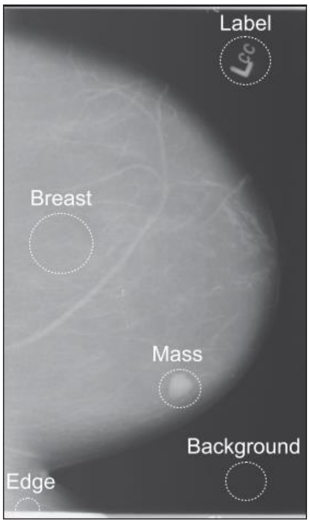

Figure 1. A typical mammogram image covered by elements from DDSM (5).

The Mask R-CNN is a standard framework for object recognition and segmentation which was proposed in different studies (10, 12). The suggested pseudocolor scheme with the Mask R-CNN deep learning architecture provides an integrated solution for mammographic mass identification and segmentation that requires no operator involvement or hand-crafted features. This study outperforms state-of-the-art algorithms using the publicly accessible Kaggle (a website with open-sourced medical datasets) environment.

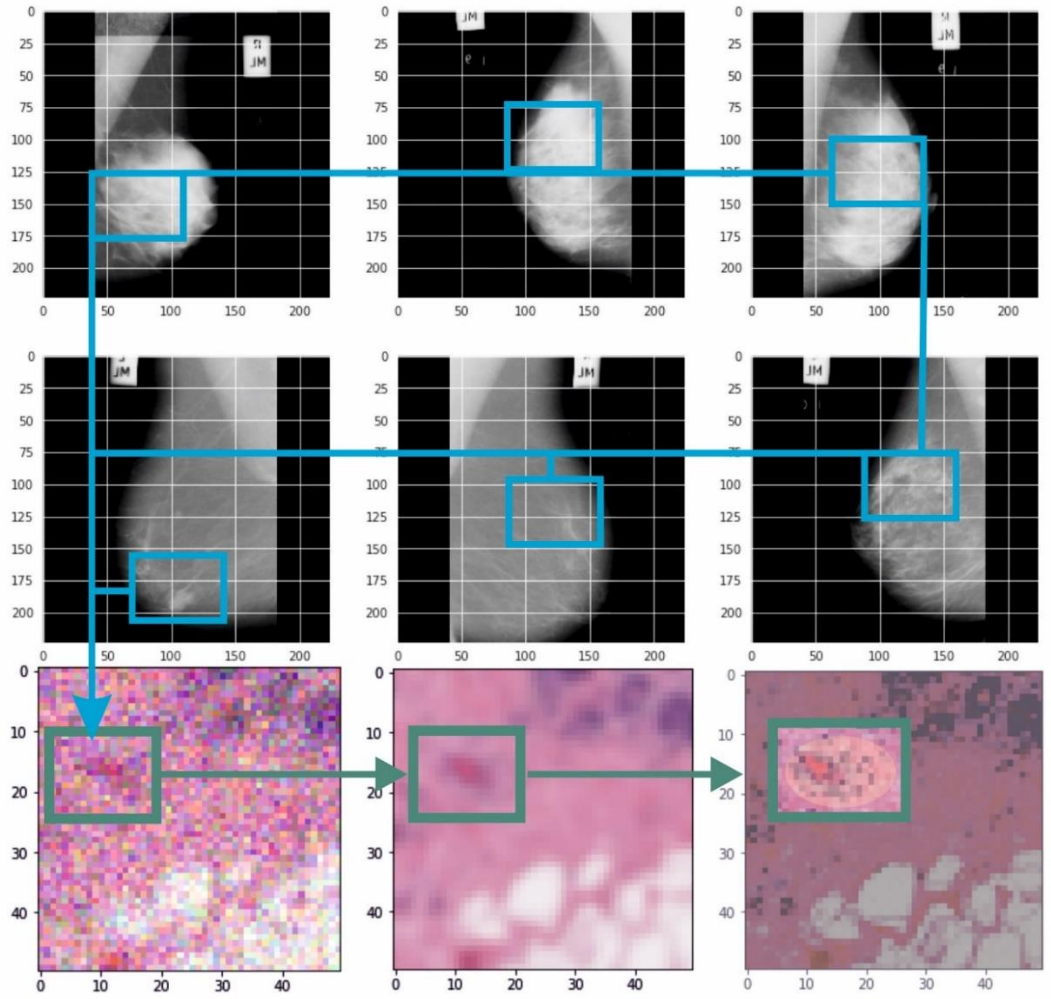

Figure 2. The planned CAD is depicted in this graphic. Multi-scale morphological sifting (MMS) is an acronym for multi-scale morphological sifting. The black outlines reflect the mass's ground truth, while the cyan outlines show the suggested method's segmentation.

Methodology

Dataset

The suggested technique is evaluated using the Kaggle dataset. This is the most extensive publicly available full-digital mammographic collection with properly annotated mammograms. There are 20 mammograms, including 100 frame capture with different axes, ranging from 16 to 256 mm2. All mammograms have a pixel standard (65px) and a bit depth of 72 bits.

Pre-Processing Applications

Thresholding isolates the breast region, and the unnecessary backdrop is cut away (13). The mammography is then padded into a square form and normalized to 16-bit. The mammography is subsampled to 1/4 of its original size using the low-pass component of a two-level Daubechies 2 wavelet transform to standardize with the literature.

Pseudocolor Mammogram Generation

At this point, all mammography frames are transformed into a pseudocolor mammogram (PCM) to accentuate the mass-like characteristics. Figure 5 displays grayscale mammography (GM) in the first channel, with two additional photos produced by the multi-scale morphological sifter (MMS) in the second and third channels. Using morphological filters with oriented linear structuring elements (LSEs), the MMS retrieves masslike characteristics, such as linear spicules, typically identified in breast masses (Figure 4; 14, 15). The MMS is stated in Eq. (1), where an input picture F is processed other n scale by two sets of logical filters, L(M1(i),(n)) and L(M2(i),(n)). The magnitudes are M1 and M2, and the orientation of the nth LSE in each set is (ρ) = ρ (180°/N). The MMS can extract patterns with diameters in the range of [M1(i), M2(i)] on the scale i. The magnitudes M1 and M2 are determined in Eq. (2 and 3), where P is the pixel size of the original picture and S is the scaling factor in the pre-processing step, given the area range of the target for detection Amin, and Amax (Figure 3).

$$MMS = \sum_{n=0}^{N-1}\{F - [F^{\circ}L\,(M_2(i),\rho(n))]\}^{\circ}L(M_1(i),\rho(n)) \quad (1)$$

$$M_1(i) = {}^{2}/_{P.S}\left(\frac{A_{min}}{\pi}\right)^{0.5}.\left(\frac{A_{max}}{\pi}\right)^{\frac{0.5(i-1)}{l}} \quad (2)$$

$$M_2(i) = {}^{2}/_{P.S}\left(\frac{A_{min}}{\pi}\right)^{0.5}.\left(\frac{A_{max}}{\pi}\right)^{\frac{0.5.i}{l}} \quad (3)$$

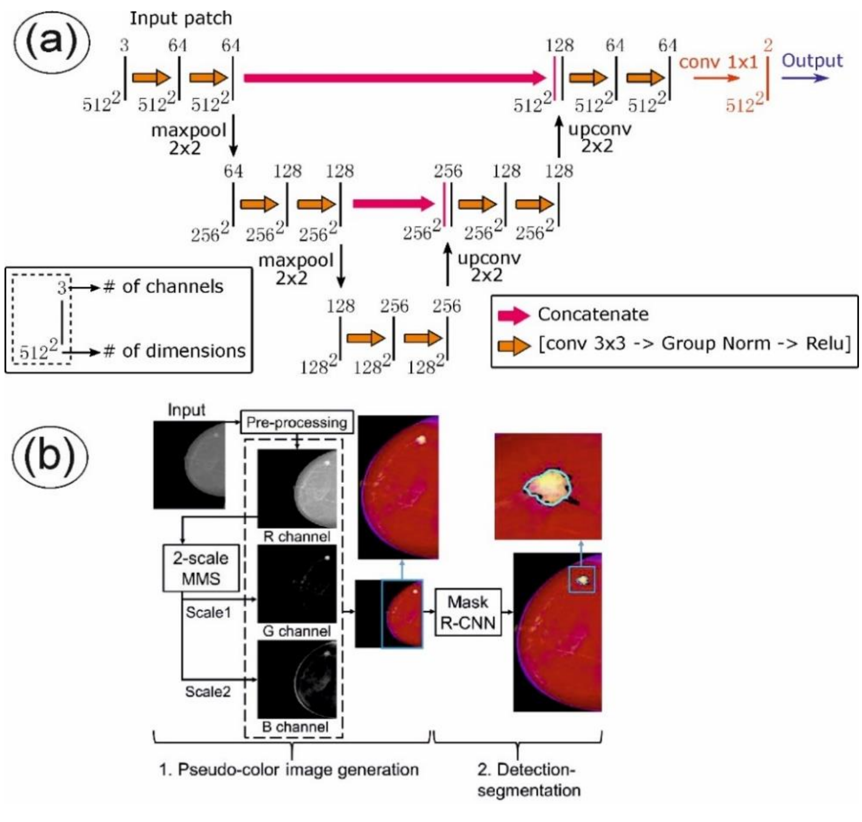

Figure 3. (a) Filter model of the R-CNN consisted on this study and (b) diagram of the network architecture of Mask R-CNN.

Four scales (I = 4) are used for the MMS (I = 4), the mass size range of Amin and Amax is recommended in Carneiro et al. and Chiao et al. as 16 to 256 mm2, respectively, with the number of LSEs (N) in each scale, is set to the default value 48 (10, 12). As defined in the pre-processing step, the resampling factor S = 1 is employed. The GM and both output images are 8-bit linearly scaled. A PCM consists of the GM in the P (purple) channel, as shown in Figure 5. This pseudocolor rendering method helps improve mass-like patterns by establishing color contrast between the mass and the backdrop when three channels are combined.

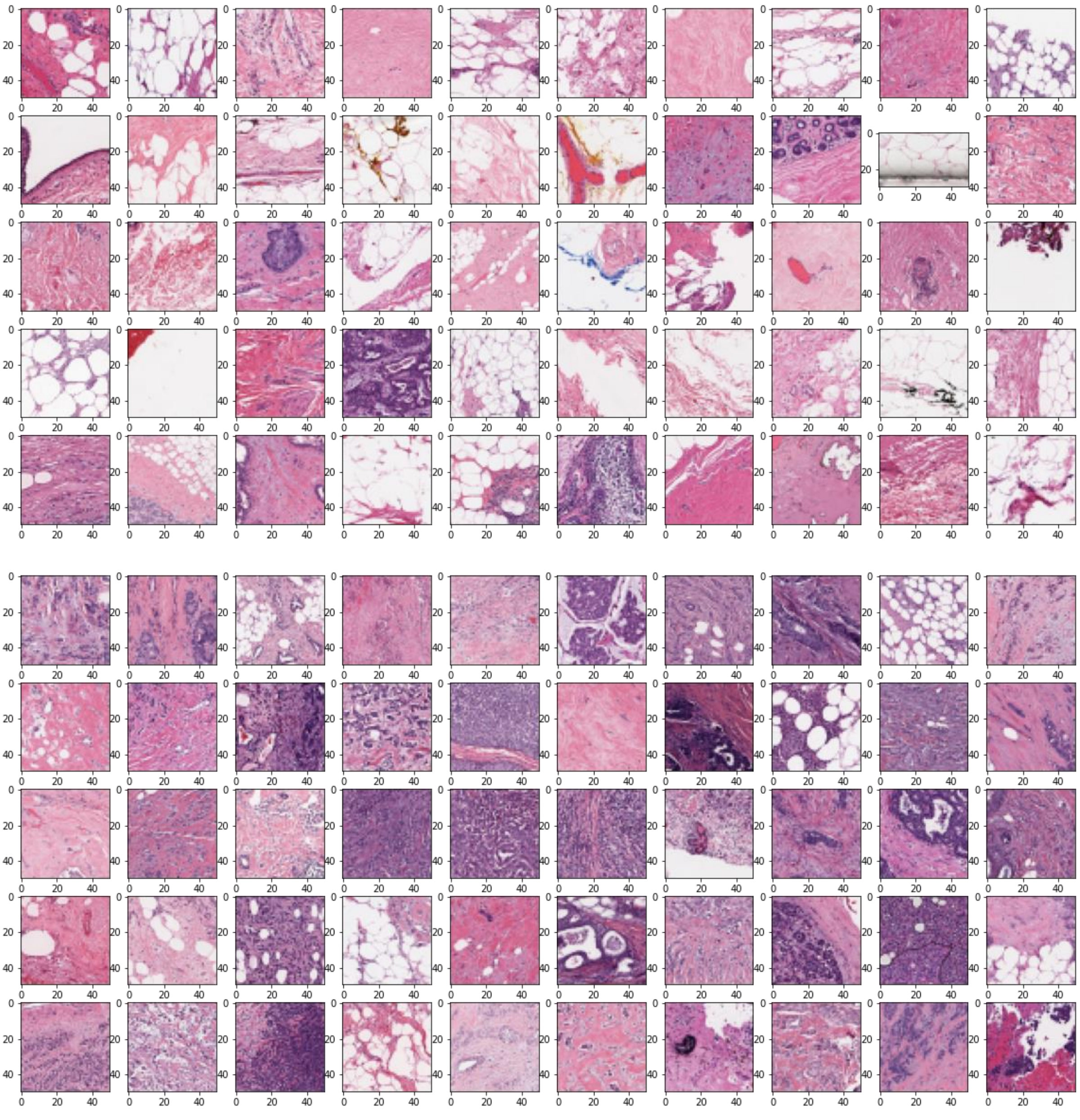

Figure 4. 100 mammogram frames cropped and filtered from 20 mammogram images after denoising and enhancments. Patches with pinky or purple accumulations could have cancer cells look more violet and crowded than healthy ones.

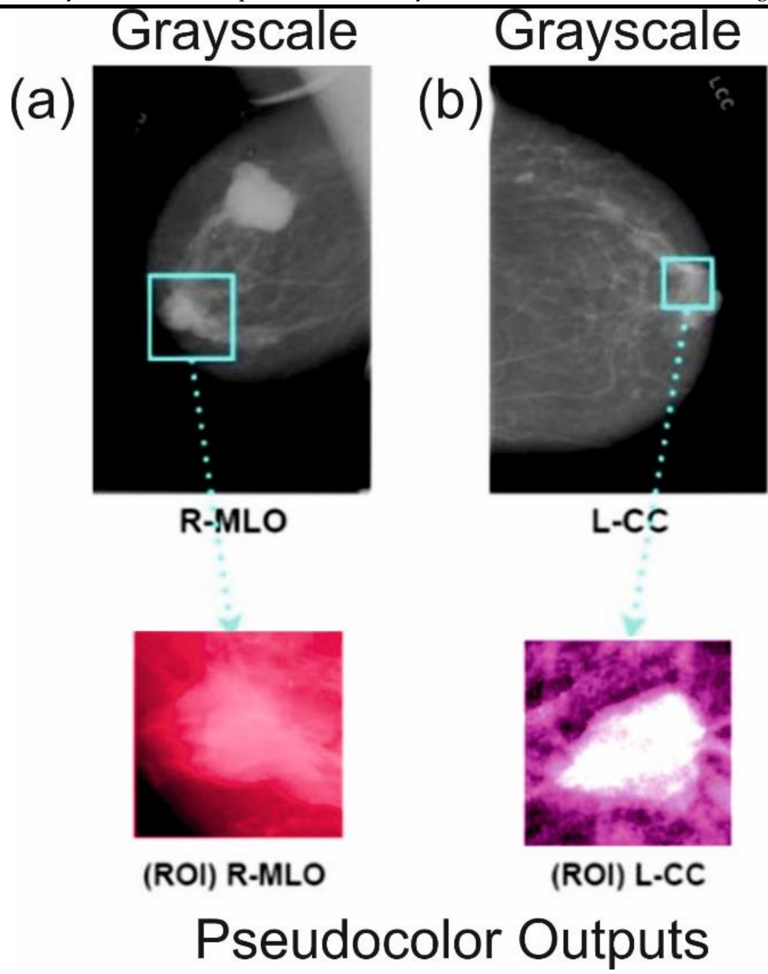

Figure 5. Pseudo-color improvement for masses in diverse sizes. (a) demonstrations a minor assembly with the exact width of 16 mm, and (b) designates a bulky assembly with a width of 256 mm.

Applying R-CNN

Because the mammographic dataset is limited, transfer learning with a pre-trained Mask R-CNN model was used in this study. The Mask R-CNN is a generic framework for body-mass recognition and segmentation simultaneously. The Faster R-CNN is used for object identification, while a fully convolutional network (FCN) is used for pixel-to-pixel segmentation. The Faster R-CNN proposes bounding box region candidates using a region proposal network, subsequently classified into distinct categories. The FCN operates in the background to segment the region candidates. Each routine of script approach takes approximately 20 minutes within one set of epochs (Figure 4), while the R-CNN model has a period on image testing with ~1 second per image. The 'Mask Rcnn' pre-trained model, developed for a binary classification issue, is used to start the Mask R-CNN training. Mask R-image CNN's resizing mode is set to 'square,' and images are shrunk to 1024 by 1024 pixels.

Results

The MMS-based PCM generation offers a novel technique to generate multi-channel inputs for DL networks like the Mask R-CNN. Using orientated LSEs, as illustrated in Figure 6, the MMS could be selectively excerpted mass-like forms and overwhelm the background. The PCM improves masses with color contrast to assist detection by merging the grayscale mammography and MMS outputs. Prior research (4, 14, 16) sought to employ a multi-channel input for CNN networks in body-mass recognition.

Compared to merely workflow GMs, PCMs improve the detection performance of Mask R-CNN. Figure 7 shows that utilizing PCMs results in a greater AUFC than GMs. Initially, 7268 blue pixels were chosen 100 frames from the DDSM with only one body mass at random. The stage of segmenting regions of interest from those images generated a total of 3871 suspected areas containing abnormalities, including 566 masses and 3305 non-masses. This level of segmentation was assessed by determining whether the mammography region linked with the mass intersected with one of the problematic regions identified by the algorithm.

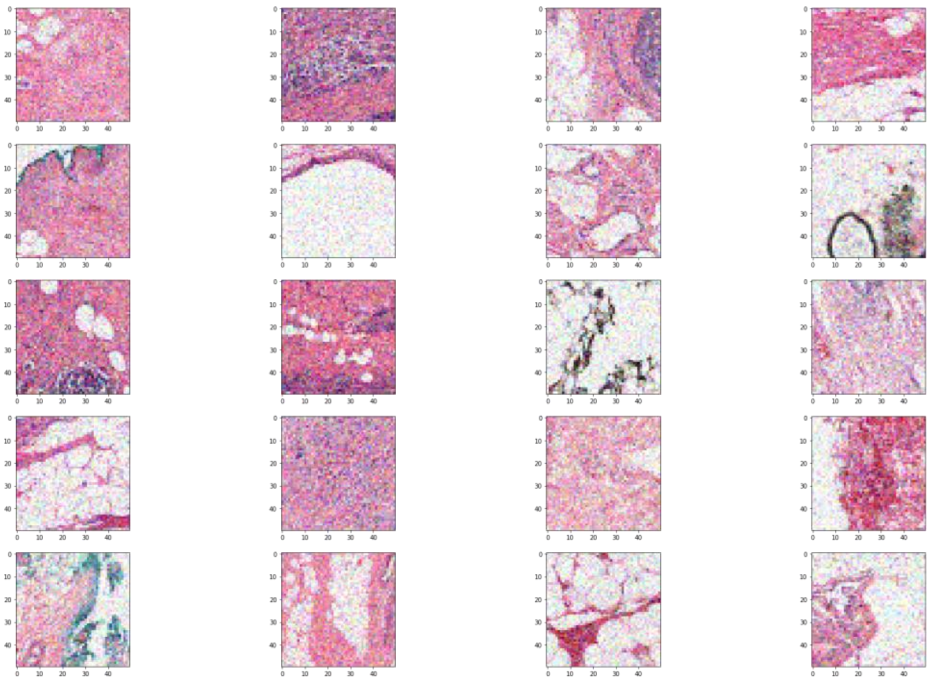

Figure 6. Detected PCM patches from different frames (in Figure 2) containing the body-mass detected by the R-CNN methodology and in/around purple is the area informed in the DDSM.

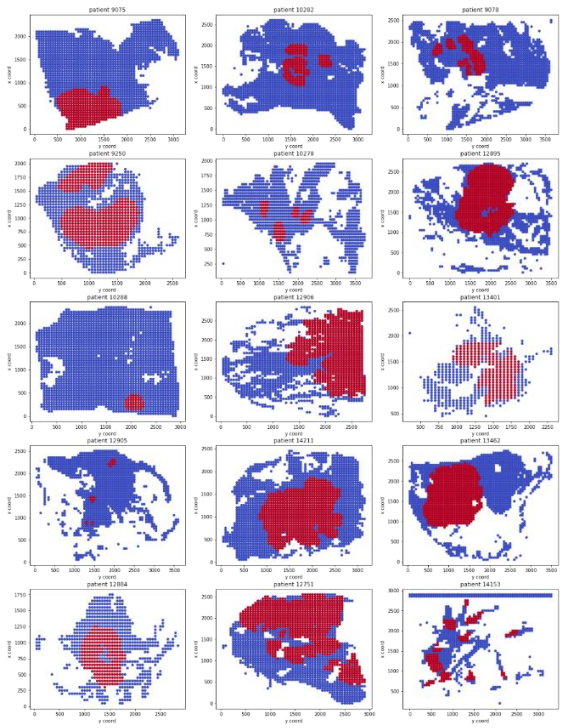

Figure 7. In given mammogram frames, after the processing covered blue areas are the regions of interest on/around purple color pigments whereas red areas are the precisely restrict the rate of color change,described as a body-mass mass according to DDSM.

Discussion

The segmentation algorithm failed to include the masses in the list of regions of interest in 17 frames depending on nine mammogram shots, accounting for ~%9 of the indications. This indicates that the parameters in the templates should be nipped to improve segmentation performance; ~65.% of the cases are represented by the 4687 pixels correctly separated or spread. These findings show that the segmentation step has good sensitivity but creates many false positives (7.1 per frame), which intend to eliminate in the classification stage. ~35.% of the mammogram captures are represented by the 2581 pixels that were incorrectly spread. These findings show that the segmentation step has good sensitivity but creates a high number of false positives – 6.7 per image intended to eliminate in the classification stage. This iterative approach still has debuts concerning the precisely estimated body mass on mammograms and model timing on these estimations. Ribli et al. have tremendous AUC rates on their classification performance (AUC:0.9), but in the meantime, their sense of the sampling rate is ten times lower than this study (17). Masses in mammograms could have amorphic structures; that's why sampling is the key to detecting these irregular pieces one on one, whereas sampling rate is the main decisive of the AUC rate. On the other hand, Agharwal and Chiao et al. describe the mass detection utilities on more than 80.000 frames via R-CNN modules (18, 12). Their accuracy on frames has more than >80.% accuracy rate and detects different geometries within this study. Although, both of the studies have more than ~1 hour estimation time to perceive any object on frames. Time is the only difference from triage to treatment to detect and subdividing any masses in mammograms. So that in this type of autonomous diagnosis, the quality of the presence is more important than the quantity. Thus, applications that can make a high number of independent definitions in a limited time, such as this study, are more in demand in medical applications.

It's worth noting that the overlay index (Ov) appears to be underperforming. Still, it's vital to remember that when mammography specialists indicate the region containing a mass, this area is frequently more significant than the actual tumor. The combination of Moran's and Geary's indices has the highest area (AUC: 0.687), but Moran's index has the smallest (AUC: 0.461) when used independently. Overall, the technique without feature reduction performed ailing when it came to classifying mass candidates. This happens when some features are redundant, unimportant, or contain a lot of noise.

Another significant circumstance depends on coefficients related to increasing model estimation. To improve the AUC level; model variants are over-sampled on considered masses, which means model breakpoints determined by R-CNN are consistent. Other drawbacks of this approach include the time it takes to perform the classification and the enormous amount of computer memory it requires, limiting the number of combinations created.

Conclusion

Based on pseudocolor mammograms with Mask R-CNN, suggested an integrated mammographic CAD for simultaneous mass identification and segmentation in this paper. Compared to grayscale mammograms, the unique pseudocolor image generating step based on MMS may offer color contrast between the masses and the background tissue, considerably improving Mask R-CNN detection performance. Hand-crafted features or user participation are not required in the proposed CAD system. The system provides exemplary performance in both body-mass recognition and segmentation in a basic framework compared to state-of-the-art approaches.

References

1. Siegel R, DeSantis C, Jemal A. Colorectal cancer statistics. CA Cancer J. Clin, 2014, 64(2): 104-17.

2. Harford J.B. Breast-cancer early detection in low-income and middle-income countries: do what you can versus one size fits all. Lancet Oncol, 2011; 12(3): 306-12.

3. Lerman C, Daly M, Sands C, Balshem A, Lustbader E, Heggan T, etal. Mammography adherence and psychological distress among women at risk for breast cancer. JNCI-J Natl Cancer I, 1993; 85(13): 1074-80.

4. Tzikopoulos S.D, Mavroforakis M.E, Georgiou H.V, Dimitropoulos N, Theodoridis S. A fully automated scheme for mammographic segmentation and classification based on breast density and asymmetry. Comput Meth Prog Bıo, 2011; 102(1): 47-63.

5. Sampaio W.B, Diniz E.M, Silva A.C, De Paiva A.C. Gattass M. Detection of masses in mammogram images using CNN geostatistic functions and SVM. Comput. Biol. Med, 2011; 41(8): 653-64.

6. Taghanaki S.A, Kawahara J, Miles B, Hamarneh G. Pareto-optimal multi-objective dimensionality reduction deep auto-encoder for mammography classification. Comput. Methods Programs Biomed, 2017; 145: 85-93.

7. Saidin N, Ngah UK, Sakim H.A.M, Siong D. N, Hoe M.K, Shuaib I.L. Density based breast segmentation for mammograms using graph cut and seed based region growing techniques. IEEE, 2010: 246-50.

8. Wang Z, Li M, Wang H, Jiang H, Yao Y, Zhang H, etal. Breast cancer detection using extreme learning machine based on feature fusion with CNN deep features. IEEE Access, 2019; 7: 105146-58.

9. Xu S, Liu H, Song E. Marker-controlled watershed for lesion segmentation in mammograms. J. Digit. Imaging, 2011; 24 (5): 754-63.

10. Carneiro G, Nascimento J, Bradley A.P. Automated analysis of unregistered multi-view mammograms with deep learning. IEEE Trans Med Imaging, 2017; 36(11): 2355-65.

11. Gan H, Li Z, Fan Y, Luo Z. Dual learning-based safe semi-supervised learning. IEEE Access, 2017; 6: 2615-21.

12. Chiao J.Y, Chen K Y, Liao K.Y.K, Hsieh P.H, Zhang G. Huang T.C. Detection and classification the breast tumors using mask R-CNN on sonograms. Medicine, 2019;98(19):e15200. doi: 10.1097/MD.0000000000015200

13. Soukup T, Davidson I. Visual data mining: Techniques and tools for data visualization and mining. New York, John Wiley & Sons, 2002.

14. Zarándy Á, Roska T, Liszka G, Hegyesi J, Kék L, Rekeczky C. Design of analogic CNN algorithms for mammogram analysis. CNNA-94 Third IEEE International Workshop on Cellular Neural Networks and their Applications IEE, 1994.

15. Costa D.D, Campos L.F, Barros A.K, Silva A.C. Independent component analysis in breast tissues mammograms images classification using lda and svm. 2007 6th International Special Topic Conference on Information Technology Applications in Biomedicine IEEE, 2007: 231-4.

16. Pereira D.C, Nascimento M.Z, Ramos R.P, Dantas R. D. Automatic detection of breast masses using two-view mammography. World Congress on Medical Physics and Biomedical Engineering, 2009: 917-20.

17. Ribli D, Horváth A, Unger Z, Pollner P, Csabai I. Detecting and classifying lesions in mammograms with deep learning. Sci. Rep, 2018; 8(1): 1-7

18. Agarwal R, Díaz O, Yap M.H, Llado X, Marti R. Deep learning for mass detection in Full Field Digital Mammograms. Comput. Biol. Med, 2020; 121: 103774.